



## Practical application of failure criteria in determining safe mud weight windows in drilling operations

R. Gholami<sup>a,\*</sup>, A. Moradzadeh<sup>a</sup>, V. Rasouli<sup>b</sup>, J. Hanachi<sup>c</sup>

<sup>a</sup> Department of Mining, Petroleum and Geophysics, Shahrood University of Technology, Shahrood, Iran

<sup>b</sup> Department of Petroleum Engineering, Curtin University, Perth, Australia

<sup>c</sup> Geological Division, Iranian Offshore Oilfield Company, Tehran, Iran

### ARTICLE INFO

#### Article history:

Received 13 September 2013

Received in revised form

12 November 2013

Accepted 20 November 2013

#### Keywords:

Mud weight windows

Failure criterion

Breakout

Fracturing

Intermediate principal stress

### ABSTRACT

Wellbore instability is reported frequently as one of the most significant incidents during drilling operations. Analysis of wellbore instability includes estimation of formation mechanical properties and the state of in situ stresses. In this analysis, the only controllable parameter during drilling operation is the mud weight. If the mud weight is larger than anticipated, the mud will invade into the formation, causing tensile failure of the formation. On the other hand, a lower mud weight can result in shear failures of rock, which is known as borehole breakouts. To predict the potential for failures around the wellbore during drilling, one should use a failure criterion to compare the rock strength against induced tangential stresses around the wellbore at a given mud pressure. The Mohr–Coulomb failure criterion is one of the commonly accepted criteria for estimation of rock strength at a given state of stress. However, the use of other criteria has been debated in the literature. In this paper, Mohr–Coulomb, Hoek–Brown and Mogi–Coulomb failure criteria were used to estimate the potential rock failure around a wellbore located in an onshore field of Iran. The log based analysis was used to estimate rock mechanical properties of formations and state of stresses. The results indicated that amongst different failure criteria, the Mohr–Coulomb criterion underestimates the highest mud pressure required to avoid breakouts around the wellbore. It also predicts a lower fracture gradient pressure. In addition, it was found that the results obtained from Mogi–Coulomb criterion yield a better comparison with breakouts observed from the caliper logs than that of Hoek–Brown criterion. It was concluded that the Mogi–Coulomb criterion is a better failure criterion as it considers the effect of the intermediate principal stress component in the failure analysis.

© 2013 Institute of Rock and Soil Mechanics, Chinese Academy of Sciences. Production and hosting by Elsevier B.V. All rights reserved.

### 1. Introduction

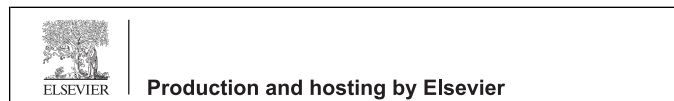
Maintaining a stable borehole is one of the major tasks in the oil and gas industry as it can induce high costs on drilling schedule (Chen et al., 2003). Wellbore stability analysis has therefore been included at the well planning stage and been studied extensively (Bradley, 1979; Bell, 2003; Zhang et al., 2003; Gentzis et al.,

2009; Zhang et al., 2009; Ding, 2011). In drilling engineering task, a linear poro-elasticity stress model in conjunction with a rock strength criterion is used to determine the optimum mud pressure required to stabilize the wellbore. During the drilling, borehole breakout and drilling induced fractures are the two main instability problems which may lead to stuck pipe, reaming operations, sidetracking, and loss of circulation. These problems can be often addressed by selecting a suitable mud weight for drilling. This is typically carried out using a constitutive model to estimate the stresses around the wellbore coupled with a failure criterion to predict the ultimate strength of reservoirs rocks. Therefore, the main aspect of wellbore stability analysis is the selection of an appropriate rock strength criterion. Numerous triaxial criteria have been proposed, which are easy to use and very common (Mohr, 1900; Fairhurst, 1964; Hobbs, 1964; Murrell, 1965; Franklin, 1971; Bieniawski, 1974; Hoek and Brown, 1980; Yudhbir et al., 1983; Johnston, 1985; Ramamurthy et al., 1985; Sheorey et al., 1989). The triaxial criteria show good agreement with the results from triaxial tests and are frequently used in stability analyses of rock structures. However, they ignore the influence of intermediate principal

\* Corresponding author. Tel.: +98 9112450994; fax: +60 85 443 837.

E-mail addresses: [Raouf.Gholami@gmail.com](mailto:Raouf.Gholami@gmail.com), [Raouf.Gholami@Curtin.edu.my](mailto:Raouf.Gholami@Curtin.edu.my) (R. Gholami).

Peer review under responsibility of Institute of Rock and Soil Mechanics, Chinese Academy of Sciences.



stress on ultimate strength of rocks, causing unrealistic prediction of stability for structures. For instance, Mohr–Coulomb strength criterion is the most commonly used triaxial criterion for determination of rocks strength. This criterion suffers from two major limitations: (a) it ignores the non-linearity of strength behavior, and (b) the effect of intermediate principal stress is not considered in its conventional form. Thus, the criterion overestimates the minimum mud pressure due to neglecting the effect of the intermediate principal stress (McLean and Addis, 1990). Vernik and Zoback (1992) found that Mohr–Coulomb criterion is not able to provide realistic results to relate the borehole breakout dimension to the in situ stresses in crystalline rocks. Zhou (1994) found that the Mohr–Coulomb criterion predicts larger breakouts because of ignoring the effect of intermediate principal stress. Song and Haimson (1997) concluded that the Mohr–Coulomb criterion did a poor job in prediction of breakout dimensions. Ewy (1999) concluded that the Mohr–Coulomb criterion is too conservative in prediction of minimum mud pressure required to stabilize the wellbore.

Hoek–Brown triaxial failure criterion is another well-known criterion successfully applied to a wide range of rocks for almost 30 years (Carter et al., 1991; Douglas, 2002; Cai, 2010). Zhang and Radha (2010) used Hoek–Brown criterion developed by Zhang and Zhu (2007) for wellbore stability analysis. They concluded that the predicted minimum mud pressure by Hoek–Brown criterion is in a better agreement with observed incidents compared to those obtained by the Mohr–Coulomb criterion. However, despite successful applications of the Hoek–Brown criterion in a number of cases, it was indicated that the intermediate principal stress needs to be included in the wellbore stability analysis (Al-Ajmi and Zimmerman, 2006).

Thus, many true triaxial or polyaxial failure criteria, such as those by Drucker and Prager (1952), Mogi (1967, 1971), Lade and Duncan (1975), Zhou (1994), Benz et al. (2008), and You (2009), have been developed to account for the effect of the intermediate principal stress in rock failure response. However, most of these criteria mathematically subject to some limitations and yield physically unreasonable solutions. For instance, the Mogi criterion (Mogi, 1971) yields two values of  $\sigma_1$  at failure for the same value of  $\sigma_2$  (You, 2009; Colmenares and Zoback, 2002). Wiebols and Cook (1968) derived a failure criterion based on shear strain energy associated with microcracks. However, this model requires the knowledge of the coefficient of sliding friction between crack surfaces which should be obtained experimentally. Furthermore, numerical methods are required for implementation of this criterion. Desai and Salami (1987) introduced a 3D failure criterion that requires more than six input parameters, and Michelis (1987) proposed another criterion in which four constants are involved (Pan and Hudson, 1988; Hudson and Harrison, 1997). In general, 3D failure criteria that contain numerous parameters or require numerical evaluation are difficult to be applied in practice, particularly for wellbore stability problems. Due to all of the above problems faced by 3D failure criteria, Al-Ajmi and Zimmerman (2005) introduced a new 3D failure criterion known as Mogi–Coulomb criterion. This failure criterion has two parameters which can be related to cohesion and internal friction angle of Coulomb strength parameters. The Mogi–Coulomb criterion does not ignore the effect of intermediate principal stress and avoids predicting unrealistic results.

In this study, to investigate the influence of the intermediate principal stress on rock failure prediction related to drilling instability, Mogi–Coulomb, Hoek–Brown and Mohr–Coulomb criteria were used. An onshore well located in southern part of Iran was used as the case study. The rock mechanical properties and magnitude of stresses were estimated from mechanical earth modeling (MEM) which is a log based analysis.

## 2. Stable mud weight window for drilling

To evaluate the stability of a wellbore, a constitutive model is required to compute the stresses around the borehole. Various constitutive models have been proposed during the past decades. Westergaard (1940) was pioneer on stress distributions around a borehole using elasto-plastic model. After that, various elasto-plastic as well as linear-elastic models have been presented for wellbore stability problems (Gnirk, 1972; Risnes et al., 1982; Aadnoy et al., 1987; Mitchell et al., 1987; Crook et al., 2002). Among the various constitutive models have been proposed, the linear poroelasticity stress model is usually used for wellbore stability analysis as it needs fewer input parameters to be determined.

Drilling process alters the states of in situ principal stresses of the formations, i.e. vertical stress ( $\sigma_v$ ) and the maximum and minimum horizontal stresses ( $\sigma_H$  and  $\sigma_h$ ), so drilling-induced stresses are introduced around the wellbore wall whose magnitudes will revert back to the in situ stresses as moving away from the wellbore wall. For isotropic elastic homogeneous rocks, borehole stresses are represented by the classical elastic solution (Kirsch, 1898), or its generalized version for nonaligned borehole and stress directions proposed by Hiramatsu and Oka (1962, 1968) and Fairhurst (1968).

Tangential, radial and axial stresses in any point around the wellbore can be defined from Kirsch's equations as

$$\sigma_\theta = \frac{1}{2}(\sigma_H - \sigma_h) \left( 1 + \frac{R^2}{r^2} \right) - \frac{1}{2}(\sigma_H - \sigma_h) \left( 1 + \frac{3R^4}{r^4} \right) \cos(2\theta) - P_w \frac{R^2}{r^2} \quad (1)$$

$$\sigma_r = \frac{1}{2}(\sigma_H - \sigma_h) \left( 1 - \frac{R^2}{r^2} \right) + \frac{1}{2}(\sigma_H - \sigma_h) \left( 1 - 4\frac{R^2}{r^2} + \frac{3R^4}{r^4} \right) \cos(2\theta) - P_w \frac{R^2}{r^2} \quad (2)$$

$$\sigma_z = \sigma_v - 2\nu(\sigma_H - \sigma_h) \cos(2\theta) \quad (3)$$

where  $\sigma_\theta$  is the tangential (hoop) stress,  $\sigma_r$  is the radial stress,  $\sigma_z$  is the axial stress induced around the wellbore at the distance  $r$  away from a wellbore with a radius of  $R$ ,  $P_w$  is the internal wellbore pressure,  $\nu$  is the Poisson's ratio of the rock, and the angle  $\theta$  is measured clockwise from the  $\sigma_H$  direction. At the wellbore wall (i.e. when  $r=R$ ), Kirsch's equations are simplified to

$$\sigma_\theta = (\sigma_H + \sigma_h) - 2(\sigma_H - \sigma_h) \cos(2\theta) - P_w \quad (4)$$

$$\sigma_r = P_w \quad (5)$$

$$\sigma_z = \sigma_v - 2\nu(\sigma_H - \sigma_h) \cos(2\theta) \quad (6)$$

According to Eqs. (4) and (6), the tangential and axial stresses are functions of the angle  $\theta$ . This angle indicates the orientation of the stresses around the wellbore circumference, and varies from  $0^\circ$  to  $360^\circ$ . Consequently, the tangential and axial stresses will vary sinusoidally. The tangential and radial stresses are functions of the pressure  $P_w$ , but the vertical stress is not. Therefore, any change in the mud pressure will only influence  $\sigma_r$  and  $\sigma_\theta$ . Inspection of these two equations reveals that both tangential and axial stresses reach a maximum value at  $\theta = \pm(\pi/2)$  and a minimum value at  $\theta = 0, \pi$ . The shear failure known as breakouts is expected to happen at the point of maximum tangential stress where the rock is under maximum compression. Tensile failure known as hydraulic or induced fracture, however, is expected to occur at the point where minimum tangential stress is applied to the rock: an

orientation 90° away from the location of shear failures around the wellbore. Reduction of mud pressure, corresponding to lower confining pressures, increases the potential for shear failure. On the other hand, increasing the mud pressure above a certain limit causes the tensile failure to happen. This discussion indicates that there is a stable window for the mud weight to drill the wellbore in a stable condition. The lower limit for this window corresponds to shear failure (breakouts) with its upper limit being the fracture initiation pressure.

The magnitudes of three principal stresses around the wellbore to analyze the initiation of induced fracture can be obtained as

$$\sigma_{\theta}^{\min} = A - P_w \quad (7)$$

$$\sigma_r = P_w \quad (8)$$

$$\sigma_z = B \quad (9)$$

$$A = 3\sigma_h - \sigma_H \quad (10)$$

$$B = \sigma_v - 2\nu(\sigma_H - \sigma_h) \quad (11)$$

For shear failure or breakouts to occur the magnitude of stresses around the wellbore are estimated as

$$\sigma_{\theta}^{\max} = D - P_w \quad (12)$$

$$\sigma_r = P_w \quad (13)$$

$$\sigma_z = E \quad (14)$$

$$D = 3\sigma_H - \sigma_h \quad (15)$$

$$E = \sigma_v + 2\nu(\sigma_H - \sigma_h) \quad (16)$$

For wellbore instability analysis, consequently, stresses at the borehole wall are the ones that should be compared against a failure criterion.

### 3. Rock failure criteria

In this section, a brief review of three failure criteria used in this study for estimation of mud weight windows in drilling applications are presented. It should be noted that in equations developed in this section for wellbore stability analysis, the pore pressure term was discarded since the stresses obtained through well log analysis will be effective stresses. Also, in this study we only consider vertical wellbores.

#### 3.1. Mohr–Coulomb criterion

Mohr–Coulomb shear failure criterion is mostly used in different engineering applications. In this criterion, shear failure takes place across a plane when the normal stress  $\sigma_n$  and the shear stress  $\tau$  across this plane are associated with a functional relation characteristic of the material (Mohr, 1900):

$$\tau = c + \mu\sigma_n \quad (17)$$

where  $c$  is the cohesion and  $\mu$  is the coefficient of internal friction of the material.

The linearized form of the Mohr failure criterion may also be written in the principal stress space as

$$\sigma_1 = \sigma_c + N\sigma_3 \quad (18)$$

$$N = [(\mu^2 + 1)^{1/2} + \mu]^2 = \tan^2\left(\frac{\pi}{4} + \frac{\varphi}{2}\right) \quad (19)$$

where  $\sigma_1$  is the major principal effective stress at failure,  $\sigma_3$  is the minimum principal effective stress at failure,  $\sigma_c$  is the uniaxial compressive strength (UCS), and  $\varphi$  is the angle of internal friction equivalent to  $\arctan \mu$ . As it was mentioned, this failure criterion

**Table 1**

Mohr–Coulomb criterion for determination of breakout pressure in vertical wellbores.

$\sigma_1 \geq \sigma_2 \geq \sigma_3$	Wellbore failure will occur if $P_w \leq P_{w(BO)}$
$\sigma_2 \geq \sigma_{\theta} \geq \sigma_r$	$P_{w(BO)} = (E - \sigma_c)/N$
$\sigma_{\theta} \geq \sigma_z \geq \sigma_r$	$P_{w(BO)} = (D - \sigma_c)/(1 + N)$
$\sigma_{\theta} \geq \sigma_r \geq \sigma_z$	$P_{w(BO)} = D - \sigma_c - NE$

**Table 2**

Mohr–Coulomb criterion for determination of fracture pressure in vertical wellbores.

$\sigma_1 \geq \sigma_2 \geq \sigma_3$	Wellbore fracture will occur if $P_w \geq P_{w(Frac)}$
$\sigma_r \geq \sigma_{\theta} \geq \sigma_z$	$P_{w(Frac)} = \sigma_c + NB$
$\sigma_r \geq \sigma_z \geq \sigma_{\theta}$	$P_{w(Frac)} = (\sigma_c + NA)/(1 + N)$
$\sigma_z \geq \sigma_r \geq \sigma_{\theta}$	$P_{w(Frac)} = (\sigma_c - B)/N + A$

assumes that the intermediate principal stress has no influence on failure and considers a linear model for obtaining the strength of the materials.

The mode of shear failure may be different depending on the order of magnitude of three principal stresses around the wellbore wall. These stresses are  $\sigma_{\theta}$ ,  $\sigma_r$  and  $\sigma_z$  presented in Eqs. (4)–(6). It has been found that the case of  $\sigma_{\theta} > \sigma_z > \sigma_r$  is the most commonly encountered stress state corresponding to borehole breakout for all in situ stresses regimes. On the other hand,  $\sigma_r > \sigma_z > \sigma_{\theta}$  is the most commonly stress regime corresponding to borehole fracture (Al-Ajmi and Zimmerman, 2005).

In shear failure case, considering  $\sigma_{\theta} = \sigma_1$ ,  $\sigma_z = \sigma_2$  and  $\sigma_r = \sigma_3$ , substituting these values in the Mohr–Coulomb failure criterion presented in Eq. (18), and introducing Eqs. (12) and (13), the lower limit of the mud pressure in order to avoid breakouts,  $P_{w(BO)}$ , will be

$$P_{w(BO)} = \frac{D - \sigma_c}{1 + N} \quad (20)$$

If the well pressure falls below  $P_{w(BO)}$ , borehole collapse will take place. Following the same procedure, the minimum allowable mud pressure to avoid breakouts around the wellbore wall corresponding to the other two possible orders of stress magnitudes can be calculated. The results of such calculations are presented in Table 1.

As discussed previously, borehole fracturing, corresponding to tensile failure of formation, will occur if the well pressure rises above the fracture initiation pressure,  $P_{w(Frac)}$ . Thus, the upper bound for mud weight windows can be calculated. Considering the order of stress magnitudes around the wellbore,  $P_{w(Frac)}$  was calculated and the results are summarized in Table 2.

It is well known that the Mohr–Coulomb criterion overestimates the tensile strength of rocks (Al-Ajmi and Zimmerman, 2005). Therefore, to use this criterion for tensile strength determination, a tensile cut-off should be considered. The tensile cut-off is defined as minimum tangential stress around the wellbore wall (Zhang et al., 2010):

$$\sigma_3 = T \quad (21)$$

where  $T$  is the uniaxial tensile strength of rock. This equation implies that if tensile failure occurs, the wellbore pressure, i.e. mud weight, should exceed the minimum tangential stress plus the tensile strength of the formation. In vertical wellbores, it is assumed that the tangential stress is the only tensile stress at the borehole wall. Introducing Eq. (7) into Eq. (21), the upper limit of the mud pressure for the tensile cut-off is obtained as

$$P_{w(cut-off)} = 3\sigma_h - \sigma_H - T \quad (22)$$

**Table 3**  
Ranges of  $m$ -values recommended for different rock types.

$m$ -values	Rock types
$5 < m < 8$	Carbonate rocks with well-developed crystal cleavage (e.g. dolomite, limestone, marble)
$4 < m < 10$	Lithified argillaceous rocks (e.g. mudstone, siltstone, shale, slate)
$15 < m < 24$	Arenaceous rocks with strong crystals and poorly developed crystal cleavage (e.g. sandstone, quartzite)
$16 < m < 19$	Fine-grained polyminerallic igneous crystalline rocks (e.g. andesite, dolerite, diabase, rhyolite)
$22 < m < 33$	Coarse-grained polyminerallic igneous and metamorphic rocks (e.g. amphibolite, gabbro, gneiss, granite, norite, quartz-diorite)

The mud pressure estimated from this equation should be compared with the value obtained for  $P_{w(\text{Frac})}$  given from those presented in Table 2. The smaller one of these values should be considered as the maximum allowable mud pressure to avoid tensile induced fracture in the formation.

### 3.2. Hoek–Brown criterion

The Hoek–Brown empirical rock failure criterion (Hoek and Brown, 1980) was developed in the early 1980s for prediction of ultimate strength of intact rock and rock masses. Over the years, the Hoek–Brown rock mass failure criterion has undergone numerous revisions (Hoek and Brown, 1988, 1997; Hoek et al., 1992, 1995, 2002). It has even been adapted to specific rock masses (Hoek et al., 1998). A summary of the changes to the Hoek–Brown failure criterion throughout its development is given by Hoek and Marinos (2007). This empirical criterion uses the UCS of the intact rock material as a scaling parameter, and introduces two dimensionless strength parameters,  $m$  and  $s$ . After studying a wide range of experimental data, Hoek and Brown (1980) stated that the relationship between the maximum and the minimum stresses at the point of failure is

$$\sigma_1 = \sigma_3 + \sigma_c \left( m \frac{\sigma_3}{\sigma_c} + 1 \right)^{1/2} \quad (23)$$

where  $m$  and  $s$  are constants dependent of the properties of the rock. The Hoek–Brown failure criterion was originally developed for estimating the strength of rock masses for applications in excavation design, but it has then been developed and used for intact rocks too.

According to Hoek and Brown (1980, 1997), the parameter  $m$  depends on rock types. Table 3 gives the ranges of  $m$ -values for different rock types.

In underground space applications, Hoek–Brown failure criterion has widely been accepted as a better criterion compared to Mohr–Coulomb criterion since it fits a non-linear model to the data, as well as provides better estimation of rock strength.

Similar calculation procedures described in the previous subsection can be used to calculate mud pressures, corresponding to the lower and upper, stable mud weight windows by assuming Hoek–Brown failure criterion. Tables 4 and 5 summarize the results. In equations presented in these tables,  $p$  and  $q$  depend on the UCS ( $\sigma_c$ ) of rocks and can be obtained using the following equations:

$$p = m\sigma_c \quad (24)$$

$$q = \sigma_c^2 \quad (25)$$

**Table 4**  
Hoek–Brown criterion for determination of breakout pressure in vertical wellbores.

$\sigma_1 \geq \sigma_2 \geq \sigma_3$	Wellbore failure will occur if $P_w \leq P_{w(\text{BO})}$
$\sigma_z \geq \sigma_\theta \geq \sigma_r$	$P_{w(\text{BO})} = \frac{(2D+p) - \sqrt{(2E+p)^2 - 4E^2 + q}}{2}$
$\sigma_\theta \geq \sigma_z \geq \sigma_r$	$P_{w(\text{BO})} = \frac{(4D+p) - \sqrt{(4D+p)^2 + 16q - 16D^2}}{8}$
$\sigma_\theta \geq \sigma_r \geq \sigma_z$	$P_{w(\text{BO})} = \frac{2(D-E) - \sqrt{4(D-E)^2 - 4(D-E-pE-q)}}{2}$

### 3.3. Mogi–Coulomb criterion

In polyaxial stress states, Mogi (1971) indicated that brittle fracture always occurs along a plane striking in the intermediate principal stress direction. He suggested a new failure criterion as below:

$$\tau_{\text{oct}} = f(\sigma_{m,2}) \quad (26)$$

where  $f$  is a nonlinear, power-law function;  $\sigma_{m,2}$  and  $\tau_{\text{oct}}$  are, respectively, the effective mean stress and the octahedral shear stress defined by

$$\sigma_{m,2} = \frac{\sigma_1 + \sigma_3}{2} \quad (27)$$

$$\tau_{\text{oct}} = \frac{1}{3} \sqrt{(\sigma_1 - \sigma_2)^2 + (\sigma_2 - \sigma_3)^2 + (\sigma_3 - \sigma_1)^2} \quad (28)$$

Parameters of this failure function cannot be easily related to the Coulomb strength parameters,  $c$  and  $\varphi$  (Colmenares and Zoback, 2002). Thus, Al-Ajmi and Zimmerman (2005) proposed that the function  $f$  can be considered to be a linear function as follows:

$$\tau_{\text{oct}} = a + b\sigma_{m,2} \quad (29)$$

where

$$a = \frac{2\sqrt{2}}{3} c \cos \varphi \quad (30)$$

$$b = \frac{2\sqrt{2}}{3} c \sin \varphi \quad (31)$$

Eq. (29) is an extension of the linear Coulomb criterion into the Mogi stress domain referred as Mogi–Coulomb failure criterion.

The strengthening effect of the intermediate principal stress can be considered by applying the Mogi–Coulomb law. The first and second stress invariants,  $I_1$  and  $I_2$ , are defined by

$$I_1 = \sigma_1 + \sigma_2 + \sigma_3 \quad (32)$$

$$I_2 = \sigma_1\sigma_2 + \sigma_2\sigma_3 + \sigma_3\sigma_1 \quad (33)$$

Using the Mogi–Coulomb criterion, we will have

$$\sqrt{I_1^2 - 3I_2} = a' + b'(I_1 - \sigma_2) \quad (34)$$

where

$$a' = 2c \cos \varphi \quad (35)$$

**Table 5**  
Hoek–Brown criterion for determination of fracture pressure in vertical wellbores.

$\sigma_1 \geq \sigma_2 \geq \sigma_3$	Wellbore fracture will occur if $P_w \geq P_{w(\text{Frac})}$
$\sigma_r \geq \sigma_\theta \geq \sigma_z$	$P_{w(\text{Frac})} = \frac{2B + \sqrt{4B^2 - 4(B^2 - pB + q)}}{2}$
$\sigma_r \geq \sigma_z \geq \sigma_\theta$	$P_{w(\text{Frac})} = \frac{(4A-p) + \sqrt{(4A-p)^2 - 16(A^2 - pA - q)}}{8}$
$\sigma_z \geq \sigma_r \geq \sigma_\theta$	$P_{w(\text{Frac})} = \frac{2(A-B) + \sqrt{[2(B-A)+p]^2 - 4[(B-A)^2 - pA - q]}}{2}$

**Table 6**

Mogi–Coulomb criterion for determination of breakout pressure in vertical wellbores.

$\sigma_1 \geq \sigma_2 \geq \sigma_3$	Wellbore failure will occur if $P_w \leq P_{w(BO)}$
$\sigma_z \geq \sigma_\theta \geq \sigma_r$	$P_{w(BO)} = \frac{1}{6-2b^2} \left[ (3D + 2b'K) + \sqrt{H + 12(K^2 + b'DK)} \right]$
$\sigma_\theta \geq \sigma_z \geq \sigma_r$	$P_{w(BO)} = \frac{1}{2}D - \frac{1}{6} \sqrt{12(a' + b'D)^2 - 3(D - 2E)^2}$
$\sigma_\theta \geq \sigma_r \geq \sigma_z$	$P_{w(BO)} = \frac{1}{6-2b^2} \left[ (3D - 2b'G) + \sqrt{H + 12(G^2 - b'DG)} \right]$
$H = D^2(4b^2 - 3) + (E^2 - DE)(4b^2 - 12), \quad K = a' + b'E, G = K + b'D$	

$$b' = \sin \varphi \quad (36)$$

The principal stresses at the borehole wall given by Eqs. (12)–(14) represent the highest stress concentration that may result in compressive failure. Introducing these equations into Eqs. (32) and (33), the first and second stress invariants will be changed to

$$I_1 = D + E \quad (37)$$

$$I_2 = DE + DP_w - P_w^2 \quad (38)$$

To determine the mud pressures corresponding to the lower and upper bounds of mud weight windows, we follow similar calculation procedures used in the two previous subsections, here, considering the Mogi–Coulomb criterion. The results are presented in Tables 6 and 7.

It is noted that the uniaxial tensile strength estimated by Mogi–Coulomb criterion is identical to that of Mohr–Coulomb criterion, since both criteria are equivalent in the state of uniaxial tension. Therefore, a tensile cut-off should also be introduced into Mogi–Coulomb failure criterion. Thus, the upper limit of the mud pressure defined by Eq. (22) should be introduced into the Mogi–Coulomb borehole failure criterion.

#### 4. Mechanical earth model (MEM)

It is well known that there are correlations between rock's physical properties obtained from petrophysical logs and its elasto-mechanical properties. For example, the larger the sonic velocity measured from DSI tool is, the larger the elastic and strength properties of the rock will be. Also, different formations with different mechanical properties subjected to a similar state of stresses may respond differently. The MEM uses this basis and extracts rock elasto-mechanical properties as well as state of stresses from data obtained in one or few wells in a field (Rasouli et al., 2011). The process includes construction of elastic property logs from physical equations, strength properties from existing correlations and then magnitude of three principal stresses in field. The extracted logs will be calibrated against core data or field test data, for example, elastic and strength properties will be checked against uniaxial

**Table 7**

Mogi–Coulomb criterion for determination of fracture pressure in vertical wellbores.

$\sigma_1 \geq \sigma_2 \geq \sigma_3$	Wellbore fracture will occur if $P_w \geq P_{w(Frac)}$
$\sigma_r \geq \sigma_\theta \geq \sigma_z$	$P_{w(Frac)} = \frac{1}{6-2b^2} \left[ (3A + 2b'N) + \sqrt{J + 12(N^2 + b'AN)} \right]$
$\sigma_r \geq \sigma_z \geq \sigma_\theta$	$P_{w(Frac)} = \frac{1}{2}A + \frac{1}{6} \sqrt{12(a' + b'A)^2 - 3(2AB)^2}$
$\sigma_z \geq \sigma_r \geq \sigma_\theta$	$P_{w(Frac)} = \frac{1}{6-2b^2} \left[ (3A + 2b'M) + \sqrt{J + 12(M^2 - b'AM)} \right]$
$J = D^2(4b^2 - 3) + (E^2 - DE)(4b^2 - 12), \quad M = N + b'D, N = a' + b'(E - 2P_0)$	

or triaxial tests data on few cores. Magnitude of minimum principal stress can also be compared against leak-off test (LOT) data if available. The logs can be calibrated, a good representative of mechanical properties and state of stresses in field. A review of the process involved in construction of MEM is given below.

#### 4.1. Elastic properties

Elastic properties including Young's modulus, shear and bulk moduli and Poisson's ratio can be estimated from three logs of compression and shear sonic ( $V_p$ ,  $V_s$ ) and density ( $\rho$ ) (Fjaer et al., 2008). However, these elastic parameters are dynamic properties obtained from log data and need to be converted to static parameters using available correlations since they are usually larger than static properties due to small strain of logging device (Fjaer et al., 2008). Numerous correlations based on various rock types have been proposed to convert dynamic to static properties, and one of them will be presented and used for the purpose of this study.

#### 4.2. Uniaxial compressive strength

Several correlations have been proposed based on studies in different fields where the UCS of rocks has been correlated with different physical properties from logs or elastic properties introduced in the previous subsection (Chang et al., 2006). One can use the correlation obtained in field which is closer to the field under study to estimate the UCS of formations. The produced log can be calibrated against core test data if any available.

#### 4.3. Internal friction angle

There have been relatively few attempts to find relationships between the angle of internal friction ( $\varphi$ ) and geophysical measurements because of the fact that even weak rocks have relatively high  $\varphi$ , and there are relatively complex relationships between  $\varphi$  and micro-mechanical features of rock such as rock's stiffness, which largely depends on cementation and porosity. Nonetheless, some experimental evidences show that shale with higher Young's modulus generally tends to possess a higher  $\varphi$  (Lama and Vutukuri, 1978). It is relatively straight forward to show that the value of  $\varphi$  in wellbore stability analysis is much less significant than UCS.

Among various correlations, the correlation proposed by Plumb (1994) was used in this study to determine the internal friction angle of formations:

$$\varphi = 26.5 - 37.4(1 - NPHI - V_{shale}) + 62.1(1 - NPHI - V_{shale})^2 \quad (39)$$

where  $NPHI$  is the notation of porosity, and  $V_{shale}$  is the volume of shale obtained by

$$V_{shale} = \frac{GR - GR_{min}}{GR_{max} - GR_{min}} \quad (40)$$

where  $GR$  is the value of gamma ray log, and  $GR_{min}$  and  $GR_{max}$  are respectively the minimum and maximum values of gamma ray log.

#### 4.4. Pore pressure

Eaton equation is conventionally used to estimate the pore pressure. While these equations were obtained from studies on shale formations, they are applied to estimate pore pressure in other formations due to the difficulty in direct measurement of pore pressure in other formations. The Eaton equation is formulated as

$$P_{pg} = OBG - (OBG - P_{pn}) \left( \frac{NCT}{\Delta t} \right)^3 \quad (41)$$

where  $P_{pg}$  is the pore pressure gradient,  $OBG$  is the overburden stress gradient,  $P_{pn}$  is the normal pore pressure (also known as hydrostatic pressure),  $\Delta t$  is the compressional wave transit time (also called slowness), and  $NCT$  is the normal compacted trend line

obtained by fitting a linear or non-linear curve to compressional wave log data.

To use Eq. (41), the overburden stress is calculated using density log. The hydrostatic pressure can also be estimated based on

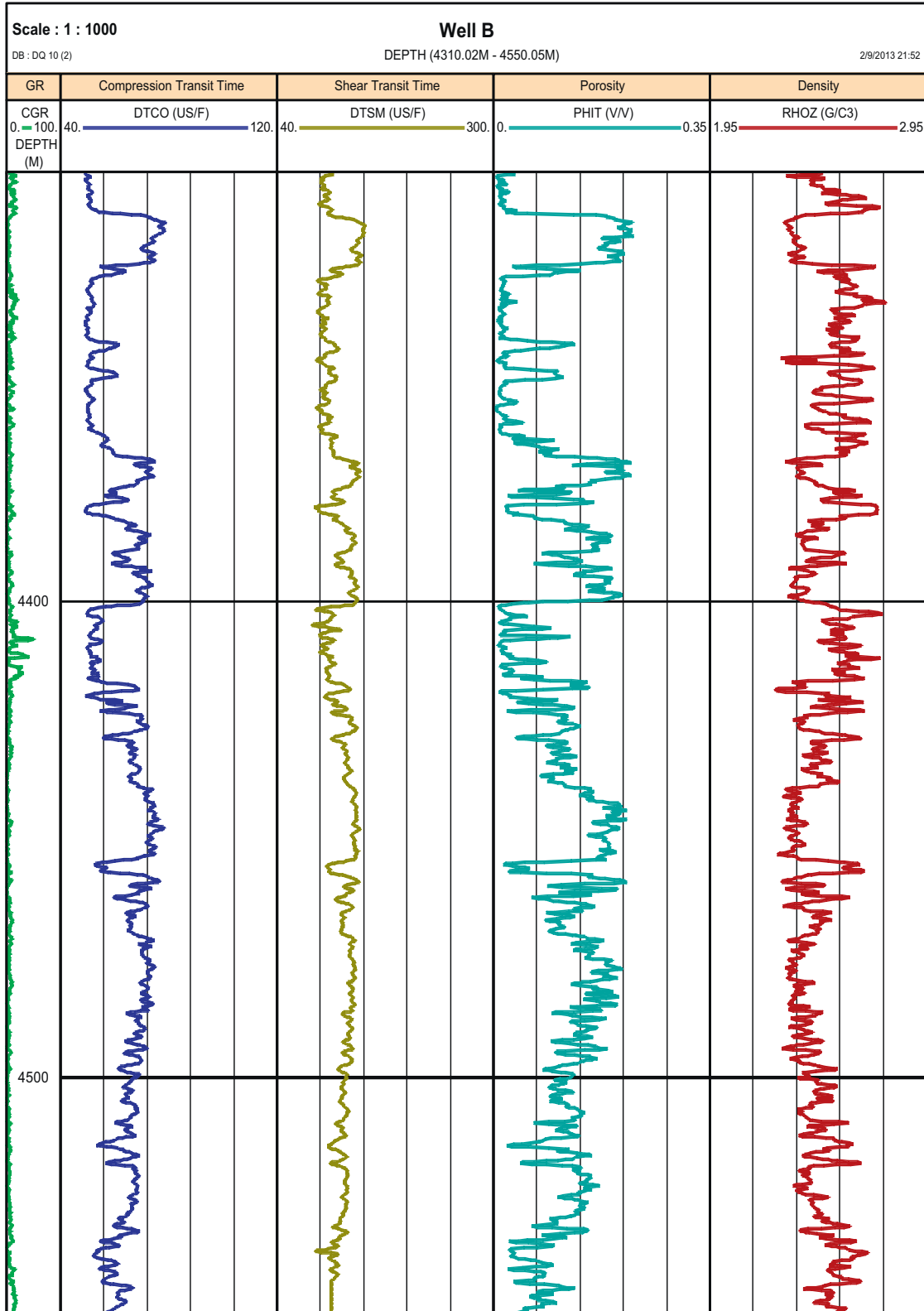


Fig. 1. Conventional well log data of Well B used for the purpose of current study.

assumption of brine density since after reaching an approximate depth of 90 m, brine is replaced with fresh water in subsurface layers due to decomposition and solution of minerals (Zhang, 2011).

#### 4.5. *In situ* stresses

Vertical stress is assumed to be a principal stress, and is usually considered to be solely due to the weight of the overburden. That is:

$$\sigma_v = \rho gh \quad (42)$$

where  $\rho$  represents the average mass density of the overlying rock,  $g$  is the acceleration due to gravity, and  $h$  is the depth. If the density varies with the depth, the vertical stress is determined by integrating the densities of the overlying rocks. At the depths of interest in petroleum exploration, the vertical stress has a gradient in the range of 18.1–22.6 kPa/m (0.8–1.0 psi/ft) (Fjaer et al., 2008). As the density log is usually acquired across the reservoir interval, extrapolation of this log toward the surface is performed to have an estimation of densities for overlying layers.

In isotropically and tectonically relaxed areas, the minimum and maximum horizontal stresses are the same. However, the horizontal stresses are not equal where major faults or active tectonics exist, which is likely the case. In this study, the poroelastic horizontal strain model (Fjaer et al., 2008) was used to determine the magnitudes of the minimum and maximum horizontal stresses. Formulations of this model are expressed as

$$\sigma_h = \frac{\nu}{1-\nu}(\sigma_v - \alpha P_p) + \alpha P_p + \frac{E_{sta}}{1-\nu^2}(\varepsilon_x + \nu\varepsilon_y) \quad (43)$$

$$\sigma_H = \frac{\nu}{1-\nu}(\sigma_v - \alpha P_p) + \alpha P_p + \frac{E_{sta}}{1-\nu^2}(\varepsilon_y + \nu\varepsilon_x) \quad (44)$$

The minimum horizontal stress obtained from above formulae can be calibrated against direct measurements of extended leak-off test (XLOT), standard LOT, or mini-frac test with a wireline tool (Yamamoto, 2003; Zoback et al., 2003). LOTs are typically performed at each casing shoe to determine the maximum mud weight possible for the next drilling interval. These LOTs, if undertaken correctly, are inexpensive but will provide calibration points for log-derived minimum horizontal stress. In fact, this test is the most commonly used method to interpret and calibrate the minimum stress magnitude (Baumgartner and Zoback, 1989; De Bree and Walters, 1989; Sarda et al., 1992; Addis et al., 1998).

## 5. Case study

In this section, the data corresponding to a well is used to construct the MEM and then the stable mud weight window is determined using three different failure criteria mentioned in Section 3. This well, Well B, is an onshore well and due to confidentiality purposes, we are unable to release the name of the field or well. However, this well is located in southern part of Iran.

### 5.1. Geology of the study area

This study uses the data belonging to an oilfield located in the Iranian Province of Kuzestan, onshore of the Ahwaz region, near the Iran–Iraq frontier. The field is a north–south oriented gentle anticline, located in the Dezful Embayment, which is a sector associated with the closing of the Neo-Tethys Sea and the Tertiary formation of the Zagros-Taurus Mountains. The oilfield is close west to the Basrah area. The structures in the Basrah area consist of gentle anticlines showing a north–south general trend which is the same to this field. The trend of these anticlines follows the old north–south oriented basement lines. The presence of Precambrian and early Cambrian salt in Northern Persian Gulf area and Saudi Arabia is considered as a reason to explain the possible origin of these structures. However, the development of these anticlines seems related to the reactivation of basement faults which can be responsible for their structural evolution. The structural growth of the field area may have already started during the Mesozoic Era or earlier and continue through the time.

The Fahliyan formation is well exposed in the Zagros Mountains in Fars Province (James and Wynd, 1965). At the same time of the sedimentation of the Fahliyan, in the area located between the oilfield and the Khuzestan Province, the intra-shelf basin of the Garau formation takes place. The current oilfield area at the time of the Fahliyan sedimentation must belong to an articulate carbonate ramp complex, partly controlled by local tectonics, partly by sea level changes, probably limited eastward by a more subsiding area that has undergone a deeper sedimentation. Argillaceous limestones and shales of deep environment are also developed in offshore Kuwait, suggesting that this area belongs to the same intra-shelf basin. The sedimentation of these units is related to the significant sea level rise that started during the late Tithonian and continued to the early Berriasian (Sadooni, 1993). The shallow water sequences of Fahliyan and equivalent units of northern Persian Gulf underlay the shale and bioclastic limestone of the Ratawi formation.



Fig. 2. View of bulk sample from Well B used to acquire plugs for rock mechanical tests.

5.2. Onshore well

Complete well log datasets, including compressional and shear sonic log, density log, neutron porosity log, caliper log as well as

resistivity log, have been acquired during the drilling phase of this well. These logs are used to study the quantitative relationships between acoustic and litho-petrophysical properties and to support seismic lithology activities (both inversion and calibration) in

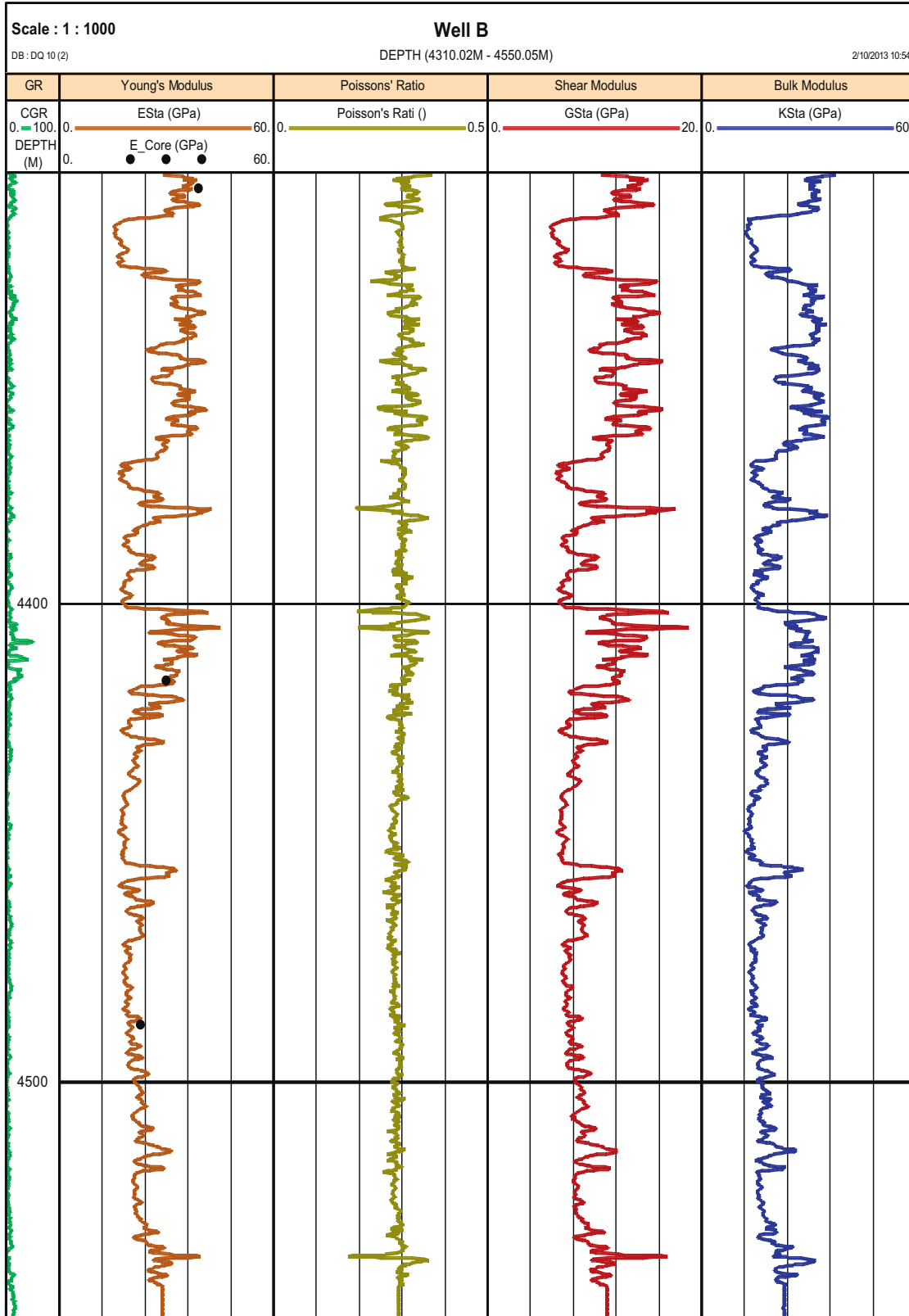


Fig. 3. Estimated elastic properties of formations in Well B.



field. At the same time, a set of acoustic and petrophysical curves, including the generated synthetic seismograms, is used to correlate well and seismic information. However, in this study, we used these logs to estimate the optimum safe mud window for drilling wells in this field using MEM. Fig. 1 shows the conventional well logs used in this study. In this figure, the first track shows the depth and the gamma ray (GR) log. The second and third tracks include compression (DTCO) and shear (DTSM) sonic logs, respectively. These are the inverse of velocities. Total porosity (PHIT) and density (RHOZ) logs are presented in the last two tracks.

Cores were acquired from depths of 4355–4550 m. The samples had been tightly bound and were transported in their original inner core barrel to maintain their integrity as much as possible. Three samples were used for mechanical tests. Fig. 2 shows the view of bulk cores used to produce plugs for the purpose of rock mechanical tests in the laboratory.

### 5.3. MEM constructed for Well B

This section presents the results of the MEM constructed for the well. Procedures described in Section 4 were used to estimate mechanical properties as well as state of stresses based on the log data and information available.

Dynamic elastic parameters of reservoir rocks were estimated using dynamic elastic equations. These parameters were then converted to static parameters using the correlation proposed by Eissa and Kazi (1988).

Fig. 3 shows the estimated log based elastic parameters of this well. The first track in this figure is the depth and GR log. The second track shows the static Young's modulus where the corresponding lab test results are shown as black circles. A good agreement between the log based and lab test results indicates the validity of the estimated property. The third track is the calculated Poisson's ratio. The fourth and fifth tracks show static shear (GSTAT) and bulk (KSTAT) moduli, respectively.

To estimate the UCS of reservoir rock, the correlation proposed by Christaras et al. (1997) was used. This correlation is formulated as

$$\sigma_c = 9.95V_p^{1.21} \quad (45)$$

To calibrate the results presented by the above correlation, UCS tests were conducted on the three core samples. To do this, sample was prepared according to the ISRM suggested methods (ISRM, 1983). However, because of the size of the core sample and preparation issues, it was impossible to prepare samples with length to diameter ratio ( $L/D$ ) of 2–2.5 as suggested by the ISRM. The samples tested had length to diameter ratio of 1. Therefore, the results were corrected using the following equation (Pariseau, 2007):

$$C = C_1 \left( 0.78 + 0.22 \frac{1}{L/D} \right) \quad (46)$$

where  $C_1$  is the unconfined compressive strength of a sample with  $L/D = 1$ , and  $C$  is the real unconfined compressive strength expected to be obtained for a sample with  $L/D = 2-2.5$ . Fig. 4 shows the view of one of the core samples prepared and used for the UCS test.

To estimate the friction angle, Eq. (39) was used and the result was presented. Next, the pore pressure and in situ stress profiles were estimated. The variation of pore pressure was determined using Eq. (41). The pore pressure log was calibrated using modular dynamic formation tester (MDT) data.

The magnitudes of in situ stresses were estimated using Eqs. (42)–(44). The LOT data were used to calibrate the magnitude of the minimum horizontal stress. The failures observed from caliper logs were used to fix the magnitude of the maximum horizontal stress. Fig. 5 presents the pore pressure and stress profiles. The first track in this figure is the depth and GR log. The second track shows the UCS log, suggesting a good agreement with the UCS test data. The third track is pore pressure (PP) profile and the fourth track is the internal friction angle log. The last track includes the magnitude of vertical ( $\sigma_v$ ), minimum ( $\sigma_{hmin}$ ) and maximum ( $\sigma_{Hmax}$ ) horizontal stresses. From this figure it is seen that the reverse fault is the dominant stress regime in this field as the order of magnitude of in situ stresses is  $\sigma_v < \sigma_{hmin} < \sigma_{Hmax}$ .

Having obtained the rock elastic and strength properties as well as the magnitude of in situ stresses, it is possible to determine the stable mud weight windows for drilling purposes. As discussed in Section 3, the results may differ depending on which failure criterion is used.

As it was mentioned in Section 3.1, the most commonly observed order of magnitude of stresses around a wellbore in terms



Fig. 4. View of core sample used for UCS test (left) and sample view after the test (right).

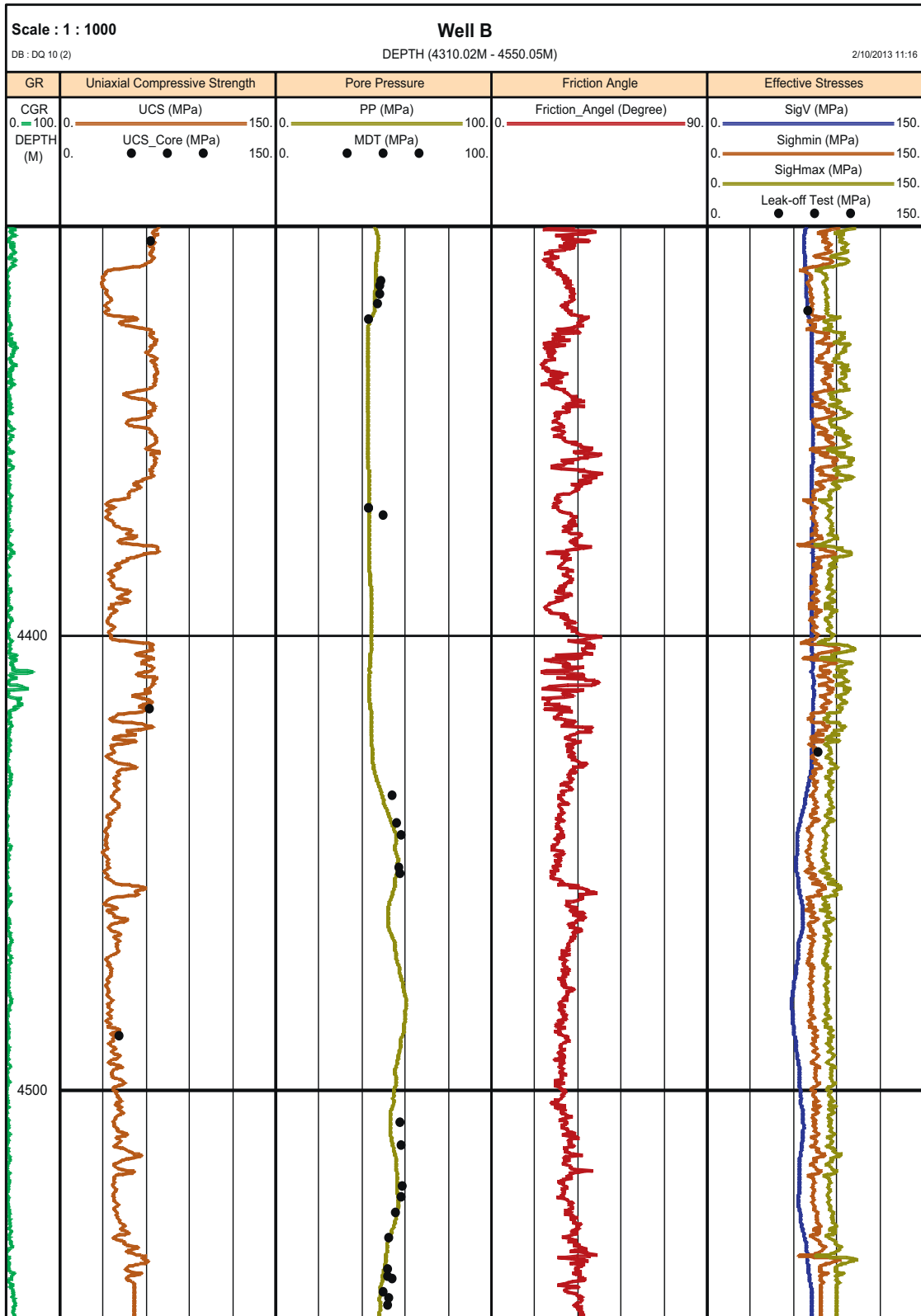


Fig. 5. Uniaxial compressive strength, pore pressure and stress profiles estimated in Well B.

of shear failure is  $\sigma_{\theta} > \sigma_z > \sigma_r$  and  $\sigma_r > \sigma_z > \sigma_{\theta}$  in case of tensile failure. Considering this assumption and the real mud weight that had been used to drill Well B (i.e.  $1.79 \text{ g/cm}^3$ ), the calculations were carried out to determine the potential for any shear failure (breakouts)

or tensile failure (induced fracture). The results of such analysis are shown in Fig. 6 considering three different failure criteria. In this figure, the first track is the depth and GR log. In the second track, the mud weight window is shown. The red profile to the left shows

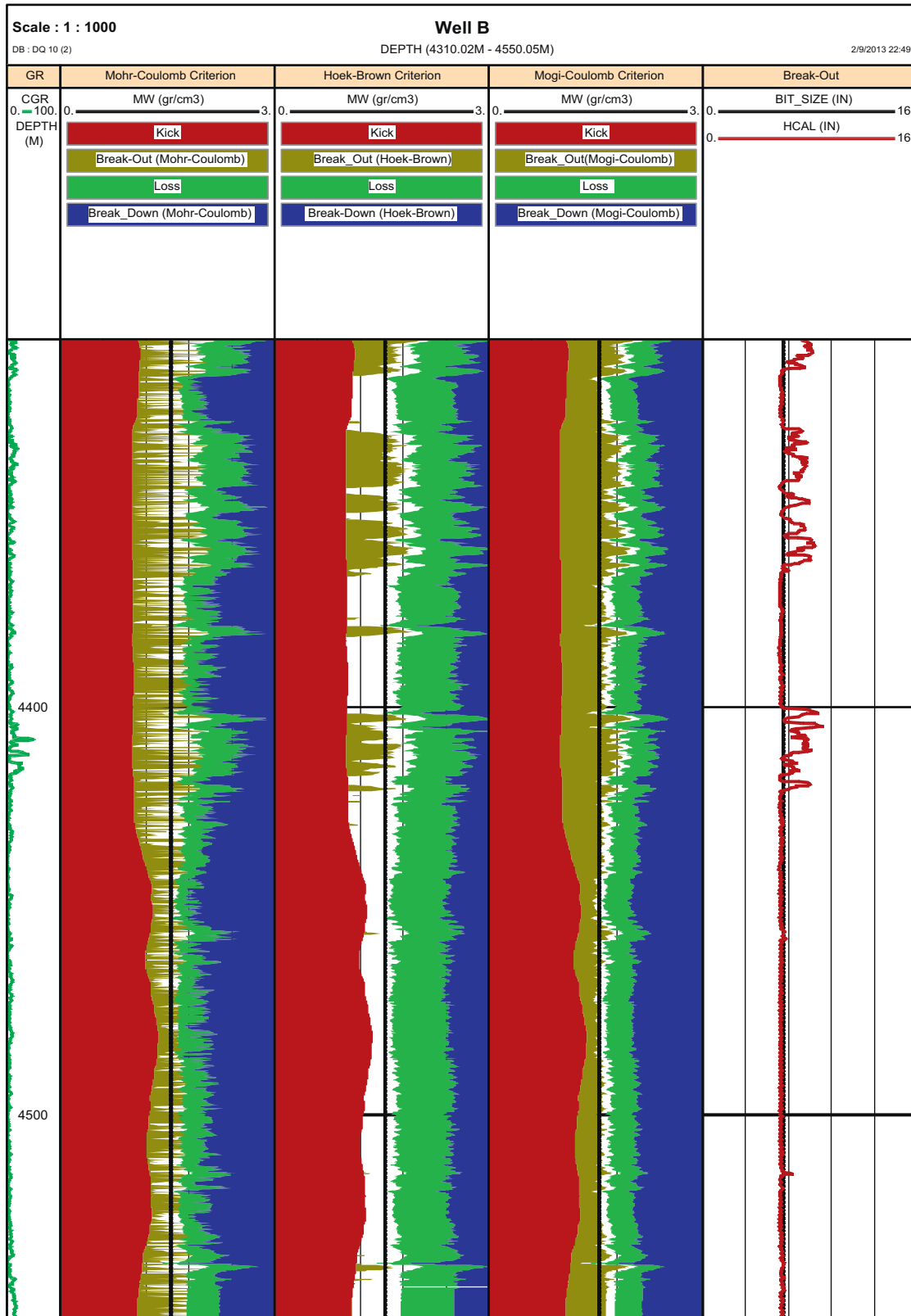


Fig. 6. Determination of stable mud weight windows for Well B using three different failure criteria.

the mud weight corresponding to kick. The brown profile is the mud weight below which breakouts or shear failure will occur. On the other side, if the used mud weight exceeds the blue or green profiles, the model predicts mud loss and induced fracture in the

formation, respectively. Therefore, the white area in the middle of track in this figure is the stable mud weight window for drilling. As is seen from this figure, this window changes as a function of depth and it is likely that this window disappears meaning that practically

there is no safe window to drill so the drill should take actions such as excessive hole cleaning when drilling in this zone. In this paper, the conclusion is different predictions obtained when using different failure criteria to determine the stable windows. In fact, a model which provides the most comparable prediction with reality is the most reliable model. The observation regarding wellbore instability or failure during drilling is captured using caliper logs or image logs such as FMI. From the caliper logs shown in this figure, severe breakouts are observed with the intervals of 4306–4314 m and 4322–4358 m as well as 4400–4421 m.

The Mohr–Coulomb criterion overestimates the rock strength and results in a larger value for the lower bound of the stable mud weight windows compared to other two failure criteria. This could be linked to the fact that in this criterion, the effect of the intermediate principal stress is ignored. Hoek–Brown and Mogi–Coulomb criteria predict the breakouts observed from caliper data more realistically; however, the latter criterion appears to give a better match with the observed failures from calipers. Thus, Mogi–Coulomb criterion perhaps is a better failure criterion to be considered for this application as it considers the effect of intermediate principal stress.

## 6. Conclusions

This study aimed at comparing the applicability of three failure criteria of Mohr–Coulomb, Hoek–Brown and Mogi–Coulomb for prediction of rock failures during drilling a wellbore. The MEM used to estimate continuous profiles of formations' mechanical properties and the state of in situ stresses is found to be a very practical and reliable tool. It was seen how the rock mechanical test data as well as field test data would help in calibration of the MEM. Determination of stable mud weight windows presented for two wells indicated that Mohr–Coulomb criterion overestimates the predicted mud weight for safe drilling. The results obtained from Mogi–Coulomb failure criterion are found to be in closer agreement with field observation compared to Hoek–Brown and Mohr–Coulomb criteria. This was related to the fact that Mogi–Coulomb criterion considers the effect of intermediate principal stress on failure prediction and this is a better representation of failure occurring in real situation.

## Conflicts of interest

There are no known conflicts of interest.

## References

- Aadnoy BS, Rogaland U, Chenevert ME. Stability of highly inclined boreholes. *SPE Drilling Engineering* 1987;2(4):364–74.
- Addis MA, Hanssen TH, Yassir N, Willoughby DR, Enever J. A comparison of leak-off test and extended leak-off test data for stress estimation. In: *Proceedings SPE/ISRM Eurock 98*; 1998. p. 131–40.
- Al-Ajmi AM, Zimmerman RW. Relationship between the Mogi and the Coulomb failure criteria. *International Journal of Rock Mechanics and Mining Sciences* 2005;42(3):431–9.
- Al-Ajmi AM, Zimmerman RW. Stability analysis of vertical boreholes using the Mogi–Coulomb failure criterion. *International Journal of Rock Mechanics and Mining Sciences* 2006;43(8):1200–11.
- Baumgartner J, Zoback MD. Interpretation of hydraulic fracturing pressure time records using interactive analysis methods. *International Journal of Rock Mechanics and Mining Sciences and Geomechanics Abstracts* 1989;26(6):461–9.
- Bell JS. Practical methods for estimating in situ stresses for borehole stability applications in sedimentary basins. *Journal of Petroleum Science and Engineering* 2003;38(3):111–9.
- Benz T, Schwab R, Kauther RA, Vermeer PA. A Hoek–Brown criterion with intrinsic material strength factorization. *International Journal of Rock Mechanics and Mining Sciences* 2008;45(2):210–22.
- Bieniawski ZT. Estimating the strength of rock materials. *Journal of the Southern African Institute of Mining and Metallurgy* 1974;74(8):312–20.
- Bradley WB. Failure of inclined boreholes. *Journal of Energy Resources Technology, Transactions of ASME* 1979;101:232–9.
- Cai M. Practical estimates of tensile strength and Hoek–Brown strength parameter  $m_i$  of brittle rocks. *Rock Mechanics and Rock Engineering* 2010;43(2):167–84.
- Carter BJ, Scott Duncan EJ, Lajtai EZ. Fitting strength criteria to intact rock. *Geotechnical and Geological Engineering* 1991;9(1):73–81.
- Chang C, Zoback MD, Khaksar A. Empirical relations between rock strength and physical properties in sedimentary rocks. *Journal of Petroleum Science and Engineering* 2006;51(3/4):223–37.
- Chen X, Tan CP, Detournay C. A study on wellbore stability in fractured rock masses with impact of mud infiltration. *Journal of Petroleum Science and Engineering* 2003;38(3/4):145–54.
- Christaras B, Mariolakkos I, Fountoulis J, Athanasias S, Dimitriou A. Geotechnical input for the protection of some Macedonian Tombs in Northern Greece. In: *The 4th international symposium on the conservation of monuments in the Mediterranean Basin*; 1997. p. 125–32.
- Colmenares LB, Zoback MD. A statistical evaluation of intact rock failure criteria constrained by polyaxial test data for five different rocks. *International Journal of Rock Mechanics and Mining Sciences* 2002;39(6):695–729.
- Crook AJL, Yu JG, Willson SM. Development of an orthotropic 3D elastoplastic material model for shale. In: *Proceedings of the SPE/ISRM rock mechanics conference*; 2002.
- De Bree P, Walters JV. Micro/minifrac test procedures and interpretation for in situ stress determination. *International Journal of Rock Mechanics and Mining Sciences and Geomechanics Abstracts* 1989;26(6):515–21.
- Desai CS, Salami MR. A constitutive model and associated testing for soft rock. *International Journal of Rock Mechanics and Mining Sciences and Geomechanics Abstracts* 1987;24(5):299–307.
- Ding DY. Coupled simulation of near-wellbore and reservoir models. *Journal of Petroleum Science and Engineering* 2011;76(1/2):21–36.
- Douglas KJ. The shear strength of rock masses. Sydney: The University of New South Wales; 2002 [PhD dissertation].
- Drucker DC, Prager W. Soil mechanics and plastic analysis or limit design. *Quarterly of Applied Mathematics* 1952;10(2):157–65.
- Eissa A, Kazi A. Relation between static and dynamic Young's moduli of rocks. *International Journal of Rock Mechanics and Mining Sciences and Geomechanics Abstracts* 1988;25(6):479–82.
- Ewy RT. Wellbore-stability predictions by use of a modified Lade criterion. *SPE Drilling & Completion* 1999;14(2):85–91.
- Fairhurst C. On the validity of the 'Brazilian' test for brittle materials. *International Journal of Rock Mechanics and Mining Sciences and Geomechanics Abstracts* 1964;1(4):535–46.
- Fairhurst C. Methods of determining in situ rock stresses at great depths. Technical report TRI-68. US Army Corps of Engineers; 1968.
- Fjaer E, Holt RM, Horsrud P, Raaen AM, Risnes R. *Petroleum related rock mechanics*. 2nd ed. Amsterdam, Netherlands: Elsevier; 2008.
- Franklin JA. Triaxial strength of rock material. *Rock Mechanics* 1971;3:86–98.
- Gentzis T, Deisman N, Chalaturnyk RJ. A method to predict geomechanical properties and model well stability in horizontal boreholes. *International Journal of Coal Geology* 2009;78(2):149–60.
- Gnirk PF. The mechanical behavior of uncased wellbores situated in elastic/plastic media under hydrostatic stress. *Society of Petroleum Engineers Journal* 1972;12(1):49–59.
- Hiramatsu Y, Oka Y. Stress around a shaft or level excavated in ground with a three-dimensional stress state. *Memoirs of the Faculty of Engineering, Kyoto University* 1962;24:56–76.
- Hiramatsu Y, Oka Y. Determination of the stress in rock unaffected by boreholes or drifts, from measured strains or deformations. *International Journal of Rock Mechanics and Mining Sciences and Geomechanics Abstracts* 1968;5(6):337–53.
- Hobbs DW. The strength and the stress–strain characteristics of coal in triaxial compression. *Journal of Geology* 1964;72(2):214–31.
- Hoek E, Brown ET. *Underground excavations in rock*. London: E & FN Spon; 1980.
- Hoek E, Brown ET. The Hoek–Brown failure criterion—a 1988 update. In: Curran JC, editor. *Proceedings of the 15th Canadian rock mechanics symposium, rock engineering for underground excavations*. Toronto: University of Toronto; 1988. p. 31–8.
- Hoek E, Brown ET. Practical estimates of rock mass strength. *International Journal of Rock Mechanics and Mining Sciences* 1997;34(8):1165–86.
- Hoek E, Carranza-Torres CT, Corkum B. Hoek–Brown failure criterion—2002 edition. In: *Proceedings of the 5th North American rock mechanics symposium*; 2002. p. 267–73.
- Hoek E, Kaiser PK, Bawden WF. *Support of underground excavations in hard rock*. Rotterdam: A.A. Balkema; 1995.
- Hoek E, Marinos P, Benissi M. Applicability of the geological strength index (GSI) classification for very weak and sheared rock masses. The case of the Athens Schist formation. *Bulletin of Engineering Geology and the Environment* 1998;57(2):151–60.
- Hoek E, Marinos P. A brief history of the development of the Hoek–Brown failure criterion; 2007 <http://www.rocksience.com/hoek/references/H2007.pdf>
- Hoek E, Wood D, Shah S. A modified Hoek–Brown failure criterion for jointed rock masses. In: Hudson JA, editor. *Proceedings of the international ISRM symposium on rock characterization*. London: British Geological Society; 1992. p. 209–14.

- Hudson JA, Harrison JP. *Engineering rock mechanics: an introduction to the principles*. Oxford: Pergamon; 1997.
- ISRM. Suggested methods for determining the strength of rock materials in triaxial compression: revised version. *International Journal of Rock Mechanics and Mining Sciences and Geomechanics Abstracts* 1983;20(6):285–90.
- James GA, Wynd JG. Stratigraphic nomenclature of the Iranian oil consortium agreement area. *AAPG Bulletin* 1965;71.
- Johnston IW. Strength of intact geomechanical materials. *Journal of Geotechnical Engineering* 1985;111(6):730–49.
- Kirsch EG. Die Theorie der Elastizität und die Bedürfnisse der Festigkeitslehre. *Z Ver Dtsch Ing* 1898;42(29):797–807.
- Lade P, Duncan J. Elasto-plastic stress-strain theory for cohesionless soil. *Journal of the Geotechnical Engineering Division, ASCE* 1975;101(10):1037–53.
- Lama RD, Vutukuri VS. *Handbook on mechanical properties of rocks*. Clausthal, Germany: Trans. Tech. Publications; 1978.
- McLean MR, Addis MA. Wellbore stability: the effect of strength criteria on mud weight recommendations. In: *Proceedings of the 65th annual technical conference and exhibition of SPE*. New Orleans: SPE; 1990.
- Michelis P. True triaxial yielding and hardening of rock. *Journal of the Geotechnical Engineering Division, ASCE* 1987;113(6):616–35.
- Mitchell RF, Goodman MA, Wood ET. Borehole stresses: plasticity and the drilled hole effect. In: *Proceedings of IADC/SPE drilling conference*; 1987.
- Mogi K. Effect of the intermediate principal stress on rock failure. *Journal of Geophysical Research* 1967;72(20):5117–31.
- Mogi K. Fracture and flow of rocks under high triaxial compression. *Journal of Geophysical Research* 1971;76(5):1255–69.
- Mohr O. Welche Umstände bedingendieelastizitätsgrenze und den Bruch eines Materials? *VDI-Zeitschrift* 1900;44:1524.
- Murrell SAF. The effect of triaxial stress systems on the strength of rock at atmospheric temperature. *Geophysical Journal of the Royal Astronomical Society* 1965;10(3):231–81.
- Pan XD, Hudson JA. A simplified three dimensional Hoek–Brown yield criterion. In: *Romana M, editor. Rock mechanics and power, plants*. Rotterdam: A.A. Balkema; 1988. p. 95–103.
- Pariseau GW. *Design analysis in rock mechanics*. Leiden, Netherlands: Taylor & Francis; 2007.
- Plumb RA. Influence of composition and texture on the failure properties of clastic rocks. In: *Eurocks 94, rock mechanics in petroleum engineering conference*; 1994. p. 13–20.
- Ramamurthy T, Rao GV, Rao KS. A strength criterion for rocks. In: *Proceedings of the Indian geotechnical conference, vol. 1*; 1985. p. 59–64.
- Rasouli V, Pallikathakathil ZJ, Mawuli E. The influence of perturbed stresses near faults on drilling strategy: a case study in Blacktip field, North Australia. *Journal of Petroleum Science and Engineering* 2011;76(1/2):37–50.
- Risnes R, Bratli RK, Horsrud P. Sand stresses around a wellbore. *Society of Petroleum Engineers Journal* 1982;22(6):883–98.
- Sadooni NF. Stratigraphic sequence, MICROFACIES, and petroleum prospect of the Yamama formation, lower cretaceous, southern Iraq. *AAPG Bulletin* 1993;77.
- Sarda JP, Detienne JL, Lassus-Dessus J. Recommendations for microfracturing implementations and the interpretation of micro- and pre-fracturing. *Oil and Gas Science and Technology—Revue d'IFP* 1992;47(2):179–204.
- Sheorey PR, Biswas AK, Choubey VD. An empirical failure criterion for rocks and jointed rock masses. *Engineering Geology* 1989;26(2):141–59.
- Song I, Haimson BC. Polyaxial strength criteria and their use in estimating in situ stress magnitudes from borehole breakout dimensions. *International Journal of Rock Mechanics and Mining Sciences* 1997;34(3/4), 116.e1–16.
- Vernik L, Zoback MD. Estimation of maximum horizontal principal stress magnitude from stress-induced well bore breakouts in the Cajon Pass scientific research borehole. *Journal of Geophysical Research* 1992;97(B4):5109–19.
- Westergaard HM. Plastic state of stress around a deep well. *Journal of the Boston Society of Civil Engineers* 1940;27:387–91.
- Wiebols GA, Cook NGW. An energy criterion for the strength of rock in polyaxial compression. *International Journal of Rock Mechanics and Mining Sciences and Geomechanics Abstracts* 1968;5(6):529–49.
- Yamamoto K. Implementation of the extended leak-off test in deep wells in Japan. In: *Sugawra K, editor. Proceedings of the 3rd international symposium on rock stress*. Rotterdam: A.A. Balkema; 2003. p. 225–9.
- You MQ. True-triaxial strength criteria for rock. *International Journal of Rock Mechanics and Mining Sciences* 2009;46(1):115–27.
- Yudhbir RK, Lemanza W, Prinzi F. An empirical failure criterion for rock masses. In: *Proceedings of the 5th ISRM congress*. Rotterdam: A.A. Balkema; 1983. p. B1–8.
- Zhang J, Bai M, Roegiers JC. Dual-porosity poroelastic analyses of wellbore stability. *International Journal of Rock Mechanics and Mining Sciences* 2003;40(4):473–83.
- Zhang J, Lang J, Standifird W. Stress, porosity, and failure-dependent compressional and shear velocity ratio and its application to wellbore stability. *Journal of Petroleum Science and Engineering* 2009;69(3/4):193–202.
- Zhang J. Pore pressure prediction from well logs: methods, modifications, and new approaches. *Earth-Science Reviews* 2011;108(1/2):50–63.
- Zhang L, Cao P, Radha KC. Evaluation of rock strength criteria for wellbore stability analysis. *International Journal of Rock Mechanics and Mining Sciences* 2010;47(8):1304–16.
- Zhang L, Radha KC. Stability analysis of vertical boreholes using a three-dimensional Hoek–Brown strength criterion. In: *Proceedings of the GeoFlorida 2010*; 2010. p. 283–92.
- Zhang L, Zhu H. Three-dimensional Hoek–Brown strength criterion for rocks. *Journal of Geotechnical and Geoenvironmental Engineering, ASCE* 2007;133(9):1128–35.
- Zhou S. A program to model the initial shape and extent of borehole breakout. *Computers and Geosciences* 1994;20(7/8):1143–60.
- Zoback MD, Barton CA, Brudy M, Castillo DA, Finkbeiner T, Grollmund BR, et al. Determination of stress orientation and magnitude in deep wells. *International Journal of Rock Mechanics and Mining Sciences* 2003;40(7/8):1049–76.